Three-wave-mixing spectroscopy of ZnSe/GaAs(001) heterointerfaces

M.S. Yeganeh,* J. Qi, J. P. Culver, and A.G. Yodh
Department of Physics, University of Pennsylvania, Philadelphia, Pennsylvania 19104

M.C. Tamargo
Department of Chemistry, City College of New York, New York, New York 10031
(Received 23 August 1993; revised manuscript received 14 December 1993)

Three-wave-mixing spectroscopy was used to probe the interfacial electronic structure of ZnSe/GaAs(001) heterojunctions. The interface spectra exhibit two sharp features at 2.92 and 2.72 eV. The former resonance was assigned to the E_1 transition of buried GaAs. This assignment was consistent with thickness-dependent measurements of the resonance intensity. The strong interfacial feature at 2.72 eV resulted from a virtual crossover transition connecting a resonance state of the interfacial quantum well to the ZnSe valence band. The interfacial quantum well was produced by band bending near the junction. Photomodulation second-harmonic measurements corroborate the assignment of the 2.72 eV resonance. A quantitative microscopic calculation of the relevant matrix elements suggests that the strong interfacial resonance at 2.72 eV is probably the result of a two-level nonlinear process involving *only* the quantum well resonance state and the ZnSe valence band. Finally we demonstrate that the interfacial deformation potential could not be responsible for the generation of the interfacial resonance.

I. INTRODUCTION

When two dissimilar crystals are abruptly adjoined, an interesting physical problem is generated. The interface of this system, as compared to the bulk, has an intrinsically different electronic structure that can strongly affect the physical properties of the entire material. Clearly, an important scientific task is to identify the electronic structure of the interface, understand its nature, and develop a complete microscopic model of the physical phenomena that arise at the junction. These exciting problems are of fundamental interest in their own right and their elucidation contributes further toward the technological development of electronic devices.

A buried solid interface is difficult to probe experimentally. Loosely speaking this results from the fact that conventional optical spectroscopies lack interface specificity, and traditional surface diagnostics have limited penetration depth. Second-order nonlinear optical probes on the other hand are potentially well suited for studying buried interfaces. They possess long penetration depths characteristic of most optical methods and intrinsic interface specificity characteristic of second-order optical processes. The surface sensitivity of sum-frequency (SF) and second-harmonic (SH) generation, is well established.[1] However, few SHG studies have been performed on buried solid interfaces[2–8] and even fewer have utilized the spectroscopic aspect of SHG.[3,5,6] A microscopic understanding of the role played by interfacial excitations in affecting nonlinear optical phenomena in this system class is, therefore, still evolving.

Nonlinear optical *spectroscopy* experiments on solid/solid interfaces were carried out by Heinz and co-workers on CaF_2/Si(111).[3] Here SFG and SHG measurements as a function of the fundamental photon energy were used to determine an interfacial band gap. The interesting result of this work was brought about by the interfacial bond combinations. It was found that the Ca ($4s$) and Si ($3p$) orbitals hybridize to produce bonding and antibonding bands at the interface with an energy separation well within the band gap of the CaF_2. Heinz and co-workers detected a transition between the bonding and antibonding orbitals of the interface states.

The present paper is concerned with the use of nonlinear optical spectroscopy to investigate ZnSe/GaAs heterostructures. ZnSe/GaAs(001) is an important *noncentrosymmetric* system that has received intense recent interest, primarily because ZnSe has been observed to lase near its optical band-gap energy of ~2.7 eV.[9] In contrast to CaF_2/Si(111), the interfacial phenomena of the ZnSe/GaAs(001) heterostructure arise as a result of a new band profile which supports new electronic states in the system. This band profile was determined by Kassel *et al.*[10] Their electrolyte electroreflectance measurements exhibited a weak spectral feature corresponding to a crossver transition between the valence band of ZnSe and a resonance state of a quantum well produced by band bending at the junction. In this paper we aim to understand the effect of this band bending on nonlinear optical spectroscopy. Our interfacial SHG and SFG spectra exhibited strong features at 2.72 and 2.92 eV. The latter resonance was due to the E_1 transition of buried GaAs and the feature at 2.72 eV was assigned to a virtual crossover transition between the valence band of ZnSe and a resonance state of the interfacial quantum well.

The interfacial resonance at 2.72 eV was sensitive to a variety of structural phenomena. In essence any process that modified the band profile near the junction affected

the strength of the resonance. Linear photomodulation is a simple way to alter the band profile. A weak beam of light generates electron-hole pairs (EHP) which can change the electric field in a material.[11,12] We have combined second-harmonic generation with linear photomodulation as a method of measurement to study solid/solid interfaces. The photomodulation second-harmonic generation (PSHG) technique was used to corroborate the existence of a quantum well at the ZnSe/GaAs heterointerface and to study interfacial trapping, electronic trap lifetimes, and surface reconstruction of buried GaAs.

The purpose of this paper is to present a coherent, and more complete picture of work that has been described briefly in several short publications, particularly in Refs. 5,6. The paper is organized as follows. Our samples and experimental set-up are described in Sec. II. The results of measurements probing the spatial and spectral origins of the SHG signal are discussed in Sec. III. In this section we also present a microscopic model for the quantum well states, which we subsequently use to calculate the interfacial second-order susceptibility. Using this model it is possible to distinguish the relative importance of two- and three-level nonlinear processes. A brief conclusion is presented in Sec. IV. Appendix A is devoted to a detailed calculation of the effect of strain on the SHG resonance, and a detailed computation of energy levels in the interfacial quantum well is carried out in Appendix B.

II. EXPERIMENT

In this section we describe our samples and explain the mechanism by which the interfacial quantum well arises. Then we discuss our experimental setup, including the normalization of the SHG signal using a wedge-shaped quartz plate. Finally we briefly describe our thickness-dependent and photomodulation SHG measurements.

A. Samples

Our heterostructure sample consists of an epitaxial layer of undoped ($n \leq 1 \times 10^{15}$ cm^{-3}) ZnSe(001), with thickness ranging from 50 Å to 1 μm, grown on a 0.5 μm undoped ($n \leq 5 \times 10^{15}$ cm^{-3}) GaAs film, terminated with a 2×4 surface reconstruction. The films were grown by molecular beam epitaxy (MBE) on an n^+ silicon-doped GaAs substrate in a MBE dual chamber.[13] One chamber was designed for the growth of GaAs and the other was used to grow the ZnSe overlayer. These two growth chambers were connected by ultrahigh-vacuum (UHV) transfer modules. As a result of the substantial technological interest in the ZnSe/GaAs heterostructure our samples have been relatively well characterized morphologically, chemically, and electrically.[14]

It is known that Zn and Ga diffuse across the buried interface during these growth processes.[15] The diffusion length for Ga (Zn) in ZnSe (GaAs) is about 30 Å (100 Å), so that relatively high (4×10^{19} cm^{-3}) dopant densities arise near the interface.[10] Because Zn is an acceptor in GaAs and Ga is a donor in ZnSe, their diffusion produces an intrinsic band bending at the interface (see Fig. 1). As a result of this band bending an interfacial quantum well forms in the GaAs conduction band. This type of quantum well at a heterointerface has been produced and studied in other systems.[16–18] The ZnSe/GaAs heterojunction differs from many previous observations however because the donors and the acceptors are *generated during growth by interdiffusion* across the junction. The interfacial quantum well in the ZnSe/GaAs system supports new electronic states with energies higher than the conduction band of the ZnSe.

B. Optical arrangements

The layout of the experimental apparatus and a rough schematic of the optical setup for SHG and SFG is displayed in Fig. 2. In these experiments polarized beams of laser light with frequencies of ω_1 and ω_2 illuminate the sample, and photons with frequency of $\omega_3 = \omega_1 + \omega_2$ are generated. The fundamental reflected photons are stopped by a spectral filter and monochromator and the

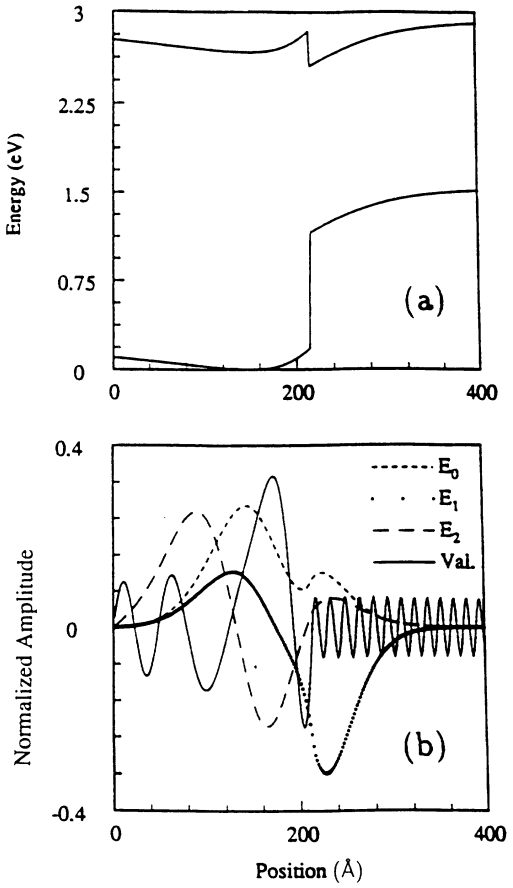

FIG. 1. (a) Energy-band profile as a function of the depth for the ZnSe/GaAs(001) system. This band profile was determined by solving the Poisson equation for a Gaussian charge distribution given in Appendix B. (b) The wave functions of the first three eigenstates of the quantum well are shown along with the valence band wave function. The thickness of the overlayer is 215 Å and z=0 is defined at the vacuum surface of the ZnSe overlayer.

intensity of the upconverted field is measured.

The fundamental light source is a Spectra Physics PDL-2 Nd:YAG pumped dye laser oscillator and amplifier system (YAG is yttrium aluminum garnet). A standard 532 nm pumped PDL-2 dye laser can cover a range from 1.38 eV (900 nm) to 2.22 eV (560 nm), but the most interesting part of the spectra in our case was in the range from 900 nm to 1000 nm. To generate such an output we have modified our PDL-2 dye laser with a new grating. This grating has 1200 lines/mm which provides an efficiency greater than 70% in the near infrared. With this grating in the oscillator the LDS925 Exciton dye can cover a range of 905 nm to 970 nm. It was determined that 144 mg/l (10 mg/l) of this dye in methanol for the oscillator (amplifier) gave optimal output power. The power spectrum of this dye is shown in Fig. 3.

In the SFG experiments the unused portion of the

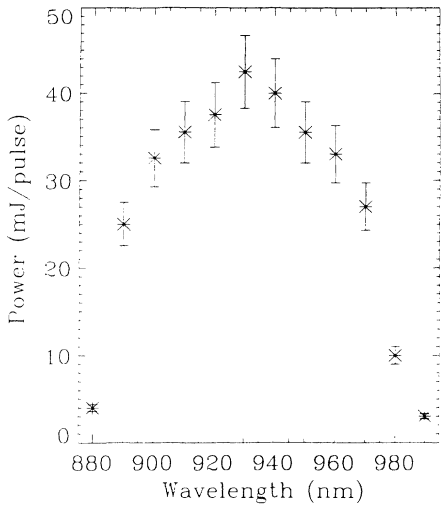

FIG. 3. Typical laser power spectrum of Exciton LDS925 dye for the modified PDL-2 dye laser. The pump power is 350 mJ/pulse at 532 nm.

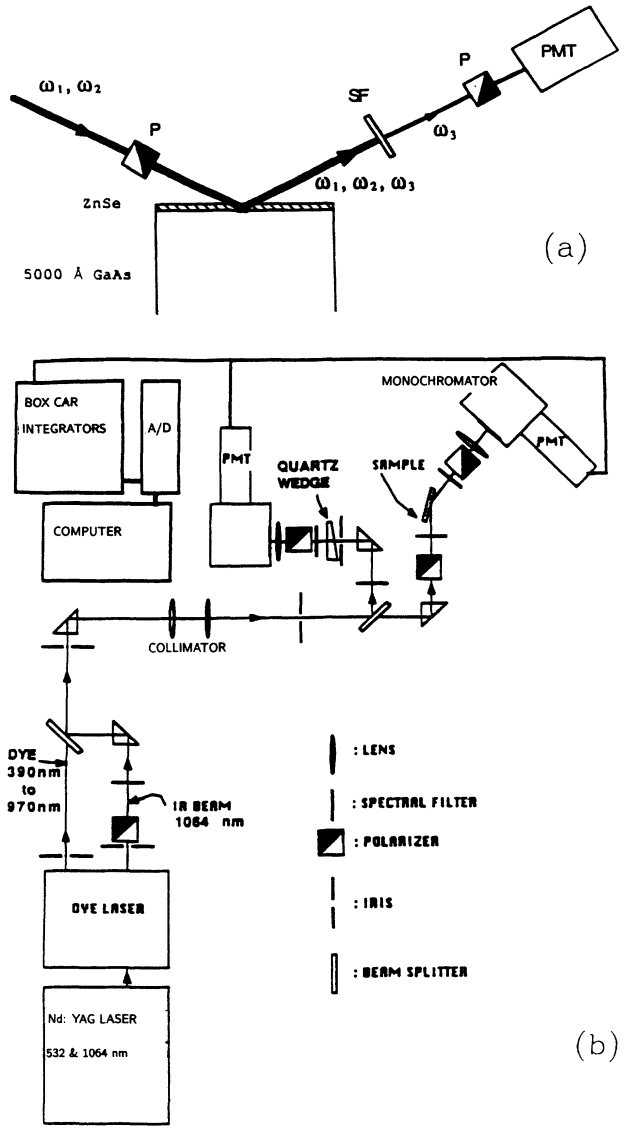

FIG. 2. (a) Schematic of SFG and SHG measurements: P, polarizer; SF, spectral filter; PMT, photomultiplier tube. (b) Optical setup for SFG and SHG measurements.

1064 nm output of the Nd:YAG laser was delayed temporally and made coincident with the dye laser output. A 10%/90% wedge-shaped fused silica plate was used to split off reference and sample beams. Normalization of the sample signal will be discussed later in this section.

The angle of incidence on the ZnSe/GaAs samples was 75°. At this angle more than 50% of the p-polarized fundamental light was transmitted into the ZnSe overlayer. The collimated beam was ~1.5 mm in diameter and had a fluence of ~5 mJ/cm^2. This fluence yielded a SHG signal on average of ~50 photons/laser pulse and a signal-to-background ratio of ~100 in a 1000-pulse average. The background signal was measured by blocking the laser beam. To attenuate the fundamental beam we used a monochromator and spectral filters. A polarizer was used to select the polarization state of the SF or SH signal before the signal reached the monochromator. The photomultipler tube output was measured and recorded using a computer and gated electronics.

Since the SH intensity is proportional to the square of the laser intensity, systematic and uncontrolled variations in laser intensity must be compensated as a function of frequency and time. To achieve this goal we measured the SH or SF intensity in transmission through a y-cut (i.e., the y axis is normal to the face of the crystal) wedge-shaped quartz plate with an apex angle of 0.8°. We used this signal to normalize the SH or SF intensity of the sample. In contrast to z-cut quartz, a y-cut quartz does not have any optical activity, and since $\chi^{(2)}_{ijk}$ of a quartz crystal does not couple to the z direction of an electric field, the birefringence property of a y-cut crystal does not affect the SHG output.

At each frequency the sample signal was normalized by the maximum SH or SF output of the reference. The maximum signal was obtained by translating the quartz wedge along a direction perpendicular to the laser beam propagation vector. We note that, because of phase

matching and interference, the transmitted SH and SF intensity of the reference sample oscillates as a function of the angle of incidence (Maker fringes[19]) and the fundamental frequency. However, the *maximum* value of the fringes generated by a small-apex-angle *wedge-shaped* quartz plate does not vary as a function of frequency.

To investigate the thickness dependence of the SHG spectra we have measured the spectra of nine ZnSe/GaAs(001) samples with different overlayer thicknesses. This method gives information about the dependence of the SHG intensity on overlayer thickness at various photon energies and provided us with more information about the spatial origin of various signals.

In the photomodulation SHG experiments we have measured the intensity of the SHG signal as a function of fluence and wavelength of a photoexciting light source. The sample was illuminated at normal incidence by light derived from either a tungsten-lamp monochromator source or an argon-ion laser, while the SHG experiment was in progress. The intensity of the photoexciting beam was $\sim 10\ \mu W/cm^2$ and never exceeded $0.5\ mW/cm^2$. Typically the sample was illuminated for a period of ~ 2 min before it reached steady state. A schematic and more details of the PSHG experiments are given in Ref. 20.

III. RESULTS AND DISCUSSION

In this section we present the SHG and the SFG experimental results and describe the methods we used to investigate the spectral and spatial origin of the signals. GaAs and ZnSe are zinc blende crystals with $\bar{4}3m$ symmetry. They both have a single nonzero bulk second-order susceptibility tensor element, $\chi^{(2)}_{xyz}$,[21,22] whose contribution to the output radiation is highly anisotropic. For the p-in/s-out polarization configuration, the bulk SHG output intensity of ZnSe/GaAs(001) is proportional to $\cos^2(2\phi)$, where ϕ is the angle between the [100] direction and the plane of incidence. The bulk SHG intensity is proportional to $\sin^2(2\phi)$ for the p-in/p-out polarization configuration. The orientation dependence of our SHG signal was reported in our earlier publication.[23] We see that by proper choice of beam polarization and sample orientation we preferentially suppress or enhance the nonlinear bulk radiation generated by the nonzero $\chi^{(2\omega)}_{xyz}$. Hereafter when we refer to interface spectra we are referring to measurements performed using the p-in/p-out polarization configuration at $\phi = 0$. Bulk spectra refer to measurements performed using the p-in/s-out polarization configuration at $\phi = 0$.

The interfacial and bulk SHG spectrum for samples of thickness 215 Å are shown as a function of upconverted photon energy in Fig. 4. Since the thickness of this sample is less than the critical thickness, the overlayer is pseudomorphic and free of misfit dislocations. The interfacial SH spectrum of this heterostructure exhibits sharp features at 2.92 and 2.72 eV. These two features were not observed directly in the bulk SH spectrum (Fig. 5).

The second-order susceptibility, and thus the second-order nonlinear signals exhibit a resonance if the photon energy of the input (fundamental) beam or output (up-

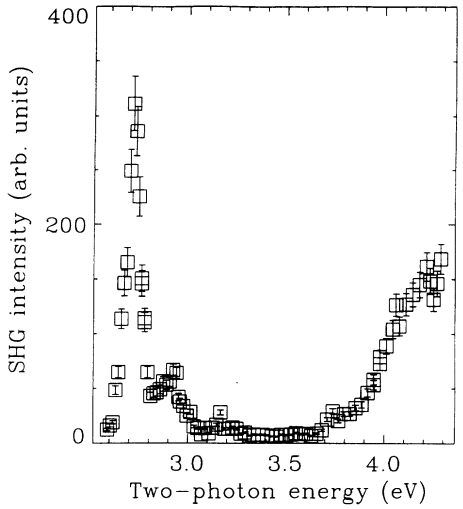

FIG. 4. Typical interfacial SH spectrum of a ZnSe/GaAs(001) heterostructure. The spectrum exhibits two sharp features at 2.92 and 2.72 eV. Thickness of the overlayer is 215 Å for this sample.

converted) beam match a transition energy in the system. The first case is termed one-photon resonance and the second case is a two-photon resonance. To identify the type of resonance, one must perform SFG and SHG experiments and compare the data as a function of one- and two-photon energy. We have compared the SFG and SHG spectra as a function of one- and two-photon energy for the sample with a 215 Å overlayer thickness in Fig. 6(a) and Fig. 6(b), respectively. It is evident that both interfacial features in the SF and SH spectra match, when the data are plotted as a function of two-photon energy. Thus, the features at 2.72 and 2.92 eV are two-photon resonances, and transitions with energy splittings of ~ 2.72 and ~ 2.92 eV are expected to exist in a

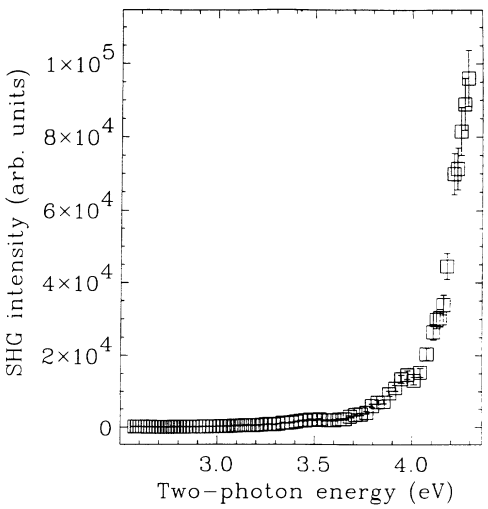

FIG. 5. Typical SH spectrum of a bulk ZnSe/GaAs(001) heterostructure. Thickness of the overlayer is 215 Å for this sample.

ZnSe/GaAs heterostructure. The transitions are termed virtual in this case because no population is transferred between the terminal states.[24] In order to obtain a better understanding of the physical phenomena giving rise to these transitions, their spatial and spectral origins must be identified.

A. Spatial origin

1. *Surface and higher-order bulk contributions*

In addition to the buried interfacial nonlinear radiation, the ZnSe front surface and ZnSe/GaAs(001) higher-order bulk nonlinearities can also contribute to the SHG and SFG *interface* signals in the p-in/p-out polarization configuration and $\phi = 0$ sample orientation. The higher-order bulk nonlinear radiation arises through magnetic dipole or electric quadrupole polarizations. It was not possible to measure the front surface and bulk contributions using thick ZnSe samples ($> 2\mu$m), because these samples exceeded the critical thickness ($\sim$ 1500 Å) of the system and were no longer pseudomorphic. Consequently, we undertook different experiments to investigate these effects.

We modified the front surface by chemical etching to check its contribution to the signal. We etched the surface using a solution of NH_4Cl in water (55 g/l) and then a solution of HCl in water (1/3 by volume). Auger electron spectroscopy and scanning electron microscopy revealed that the front surface was roughened and chemically modified. The SH spectrum of the sample, before and after chemical etching, are shown in Fig. 7. There is no detectable change in the signal.

In another experiment we sputtered the front surface with an Ar^+ beam in a UHV chamber. The SHG spectrum remained qualitatively unchanged. These results indicated that the interfacial SH signals were not very sensitive to variation of the front surface.

The isotropic contribution of the higher-order bulk nonlinearity, ζ of ZnSe/GaAs(001) was detected by a SHG experiment in the s-in/s-out polarization configuration.[25] Our data, shown in Fig. 8, indicate that the higher-order bulk anisotropic contribution was below the noise level of our system. We also have measured the contribution of the linear combination of the anisotropic higher-order bulk nonlinearity γ and interface and surface $\chi^{(2)}_{\perp\parallel\parallel}$ in the s-in/p-out polarization configuration. This contribution was ~40 times smaller than that of the interface signal, seen in Fig. 8. In summary, it is evident that the observed interface resonance signal does not originate from surface or higher-order bulk nonlinearity.

2. *Thickness-dependent measurements*

To further clarify the spatial origin of the signal and understand the difference between the 2.72 and 2.92

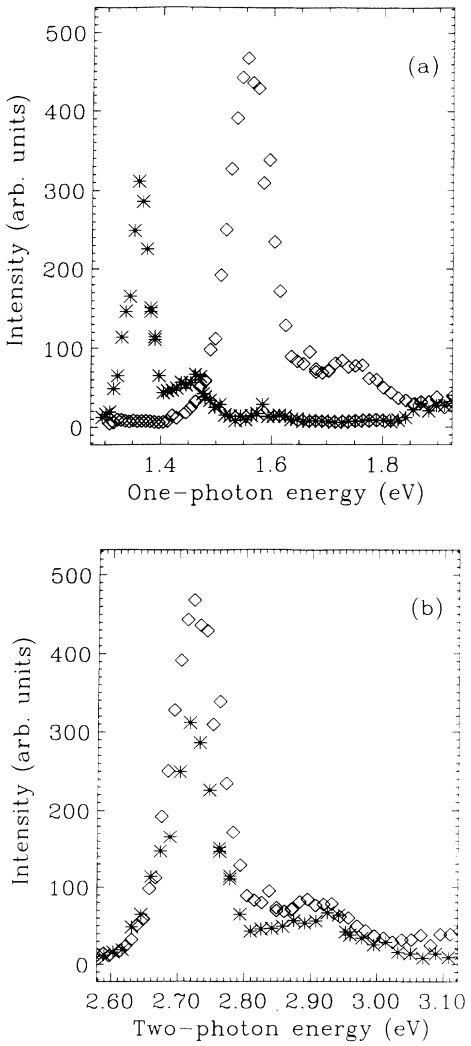

FIG. 6. Variation of SH (*) and SF (◇) intensity as a function of (a) one-photon energy and (b) two-photon energy. It is clear that both features are two-photon resonances. Thickness of the overlayer is 215 Å.

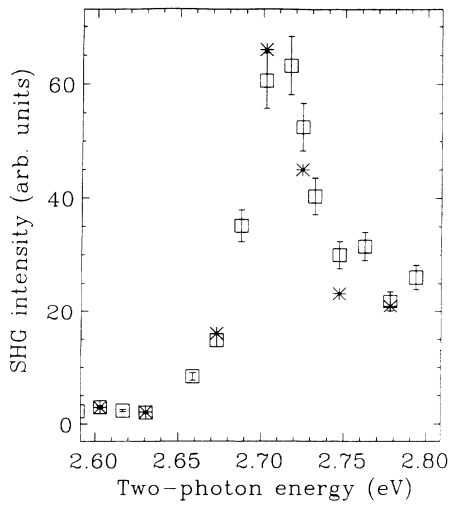

FIG. 7. Variation of SH intensity as a function of energy of the 1028 Å sample before (□) and after (*) chemical etching. The chemical etching did not produce any detectable change in the spectrum.

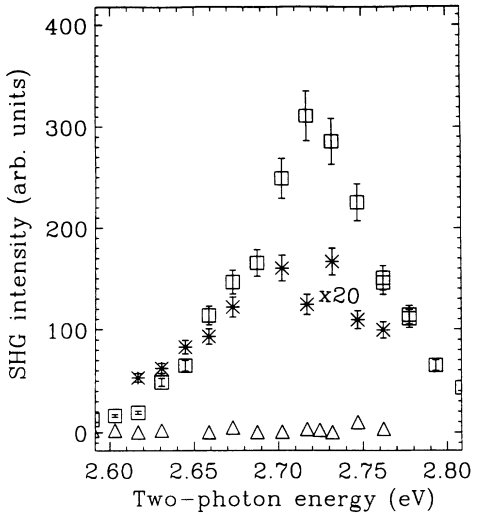

FIG. 8. Variation of SH intensity as a function of two-photon energy in the s-in/s-out ($\triangle$) and s-in/p-out ($*$) polarization configurations. The interfacial SH spectrum ($\square$) is shown for comparison. The s-in/s-out intensity is below our detection limit and the s-in/p-out peak intensity is ~40 times smaller than the interface signal.

eV resonance features, we have performed a series of thickness-dependent measurements. These experiments were motivated by the fact that *signals with different spatial origin behave differently as a function of the overlayer thickness.* To illustrate this fact we performed the following experiments.

(a). *Bulk SHG.* We have reported that the SHG signals generated through the allowed $\chi^{(2\omega)}_{xyz}$ of the *bulk* ZnSe/GaAs(001) sample *oscillate* as a function of the overlayer thickness.[23] The oscillation is a simple nonlinear optical interference effect which leads to the determination of the second-order susceptibility of the ZnSe overlayer. The second-order susceptibility of ZnSe exhibits a sharp feature at 2.67 eV. We have assigned the feature to the E_0 transition of the ZnSe bulk overlayer.

(b). *Interfacial resonance at 2.92 eV.* On the other hand, the intensity of the *interfacial* resonance at 2.92 eV *decreases* almost exponentially as the thickness of the ZnSe overlayer increases. This behavior suggests that the signal is generated in the buried GaAs and decays in the ZnSe overlayer. In this section we will describe a simple model that can predict this thickness-dependent behavior. In our model we will treat the ZnSe overlayer as a linear medium, and we assume that the SHG signal is generated at the buried interface or below the junction.

Consider the geometry shown in Fig. 9, where the ZnSe/GaAs junction is at $z = 0$ and the air/ZnSe interface is at $z = d$. d is the thickness of the ZnSe overlayer. With the beam polarization parallel to the plane of incidence (p polarization), it is straightforward to show that

$$\frac{E^{(2\omega)}_{\text{total}}}{E^{(2\omega)}_0} = t_{10}e^{i\phi_1} + t_{10}r_{10}r_{12}e^{i\phi_1}e^{i\phi_2} + t_{10}r^2_{10}r^2_{12}e^{i\phi_1}e^{2i\phi_2} + \cdots, \quad (1)$$

with

$$t_{10} = \frac{2n_1\cos\theta_1}{\cos\theta_1 + \cos\theta_0}, \quad (2)$$

$$r_{10} = \frac{n_1\cos\theta_0 - \cos\theta_1}{n_1\cos\theta_0 + \cos\theta_1}, \quad (3)$$

$$r_{12} = \frac{n_1\cos\theta_2 - n_2\cos\theta_1}{n_1\cos\theta_2 + n_2\cos\theta_1}, \quad (4)$$

$$\phi_1 = \frac{2\pi d}{\lambda}(n_1\cos\theta_1 - \cos\theta_0), \quad (5)$$

and

$$\phi_2 = \frac{4\pi d}{\lambda}\cos\theta_1 n_1. \quad (6)$$

Here $E^{(2\omega)}_0$ is the second-harmonic field, emerging from the ZnSe side of the buried junction, but generated in GaAs, and $E^{(2\omega)}_{\text{total}}$ is the total second-harmonic field

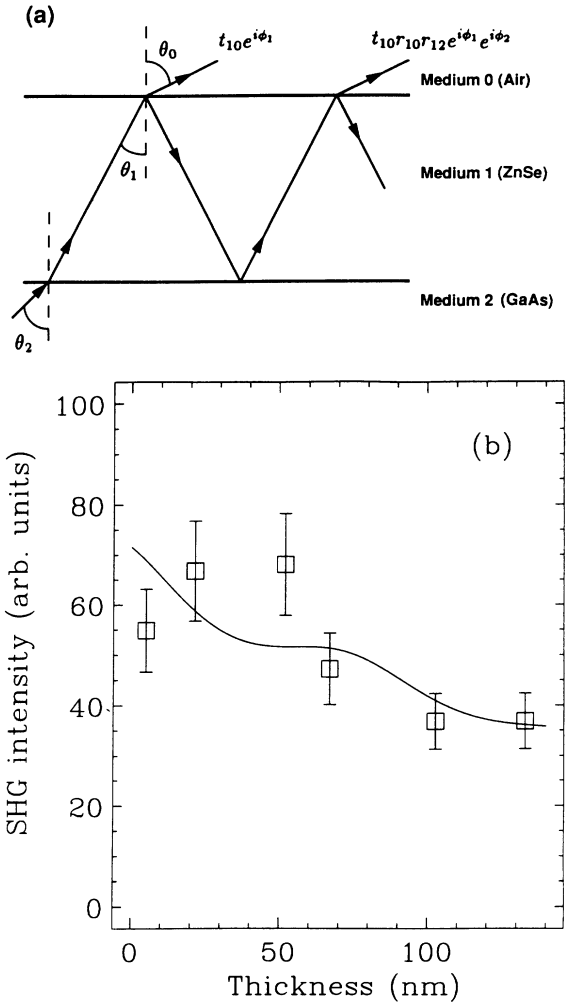

FIG. 9. (a) Simplified coordinates for the model that describes the spatial origin of the 2.92 eV resonance. (b) The 2.92 eV interfacial resonance as a function of overlayer thickness. The solid line is the prediction of the model described in the text.

emerging from the sample. n_1 (n_2) is the complex index of refraction of ZnSe (GaAs), and all angles are shown in Fig. 9(a). Equation (1) reduces to a closed form

$$\frac{E_{\text{total}}^{(2\omega)}}{E_0^{(2\omega)}} = \frac{t_{10}e^{i\phi_1}}{1 - r_{10}r_{12}e^{i\phi_2}}. \tag{7}$$

For small reflectivity Eq. (7) reduces to a *purely exponential* form. The effect of the multiple reflection is to mix the exponential decay with an oscillation. The intensity of $E_{\text{total}}^{(2\omega)}$ along with the experimental results is displayed as a function of thickness in Fig. 9(b). The theoretical curve for $E_{\text{total}}^{(2\omega)}$ was generated using the following parameters:[26,27]

$$\left.\begin{aligned} n_1 &= 2.847 + 0.145i \\ n_2 &= 4.682 + 1.933i \end{aligned}\right\} \quad \text{at } \lambda = 425 \text{ nm}.$$

The angle θ_0 is 75° and all other angles were found using Snell's law. The only adjustable parameter in this computation is the amplitude of the intensity at $d = 0$. The theoretical calculation matches the second-harmonic intensity at 2.92 eV within the experimental accuracy. This agreement suggests that the spatial origin of the interfacial resonance at 2.92 eV is in GaAs. Since the energy of this feature is consistent with the E_1 transition of GaAs,[28] we have assigned it to this transition.

(c). *Interfacial resonance at 2.72 eV.* The thickness-dependent behavior of the 2.72 eV resonance is more complicated than either of the two cases presented above. The SHG intensity as a function of overlayer thickness-is displayed in Fig. 10. The solid line is the prediction of the thickness-dependent intensity based on a model similar to the bulk, where the susceptibility was assumed to be uniform through the overlayer and GaAs was taken as a linear medium. The experimental results do not agree with the calculations. A close inspection of the data also reveals that the thickness-dependent behavior cannot be explained by the simple exponential model described in Sec. III A 2 b (see Fig. 10).

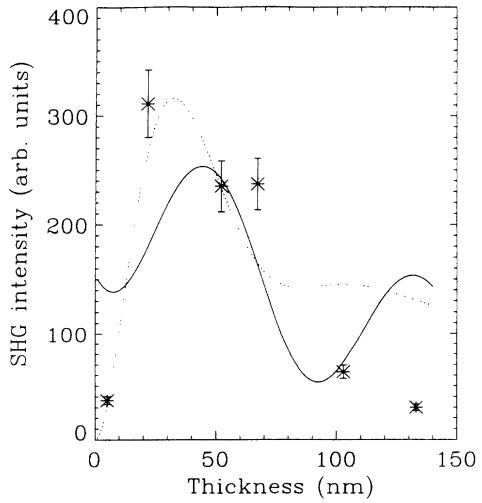

FIG. 10. Thickness dependence of the 2.72 eV interfacial resonance. The solid line is the prediction of the thickness-dependent intensity based on a model similar to the bulk, where the susceptibility is assumed to be uniform through the overlayer. The dotted line is the result of the calculation based on the model which takes $\chi^{(2)}$ as position dependent.

In another model we assumed that the susceptibility has its maximum value at the interface and decays exponentially with distance from the junction. The motivation for this model was described in Ref. 23. The result of this calculation is shown by a dotted line in Fig. 10. Even though this result is closer to the experimental results than the previous model, it still does not describe the dependence of the 2.72 eV resonance as a function of the overlayer thickness. The failure of these models to accurately predict this thickness dependence indicates that the interface signals at 2.92 eV and 2.72 eV, and the bulk signals have different spatial origins and are, most likely, intrinsically different.

B. Spectral origin

We will now discuss the spectral origin of the 2.72 eV interfacial resonance. In our ZnSe/GaAs(001) system, resonant electronic states with energy higher than the conduction band of ZnSe exist in the quantum well. Thus, *crossover* optical transitions can occur between the valence band of ZnSe and the resonance states of the interfacial quantum well. The SHG feature at 2.72 eV corresponds to a virtual[24] crossover transition between the interfacial quantum well state and the ZnSe valence band. A crossover excitation[29–31] is a transition between two states whose density of states (DOS) is provided by two spatially *separated* materials. This kind of transition can arise when the wave functions of the terminal states extend beyond the interface. Then the states can be directly coupled by photoexcitation. Ultrasensitive electrolyte electroreflectance (EER) measurements in doped ZnSe/GaAs systems have independently revealed the existence of a crossover transition.[10] This transition was always blueshifted by 40–60 meV with respect to the ZnSe E_0 transition and appears as a weak structure on the shoulder of the ZnSe E_0 peak.[10] In contrast to the EER measurements, the crossover SH resonance is a virtual transition, has nearly zero background, and possesses a nonlinearity that is comparable in magnitude to the bulk $\chi_{xyz}^{(2)}$.

In this section we will first show that the deformation potential is not responsible for the generation of the interfacial feature at 2.72 eV. Then, we present the PSHG experimental results which further establish the relation between the 2.72 eV resonance and the interfacial quantum well.

1. *The effect of the deformation potential*

The ZnSe/GaAs(001) system contains a small lattice mismatch that produces a deformation potential within the heterostructure. This deformation potential introduces a tetragonal distortion of the ZnSe unit cell and gives rise to a biaxial compressive strain in the layer. As a result, the fourfold-degenerate valence band of the

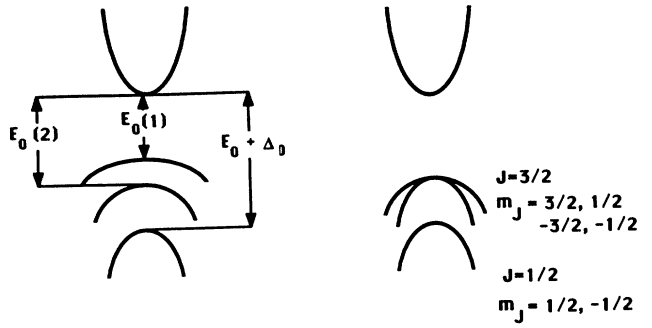

FIG. 11. Optical transitions and band splitting caused by the deformation potential near the center of the Brillouin zone.

ZnSe, Γ_8, splits into two twofold-degenerate bands.[32] The conduction bands, Γ_6 and Γ_7, cannot split, but they can shift in energy. The optical transitions and band splitting of the system are shown in Fig. 11. This mechanism will change the optical band gap of the overlayer. Under these conditions it is essential to investigate the effect of the deformation potential on the SHG signal. The deduced $\chi^{(2)}_{xyz}$ from the bulk of the ZnSe overlayer is shown, along with the interface SH intensity data in Fig. 12. The bulk resonance at 2.67 eV, corresponding to the E_0 transition, is shifted by ~50 meV with respect to the interface feature. It is natural to ask if the SHG signal at 2.72 eV is the bulklike signal localized near the interface with a shift in energy resulting from the deformation potential. To answer this question we have computed the shift in band-gap energy of ZnSe as a function of the strain in Appendix A. The measured energy shift is ~ 4 times too large to be attributed to the measured strain in the system. Therefore it is unlikely that the deformation potential is responsible for the shift between the bulk and interface features.

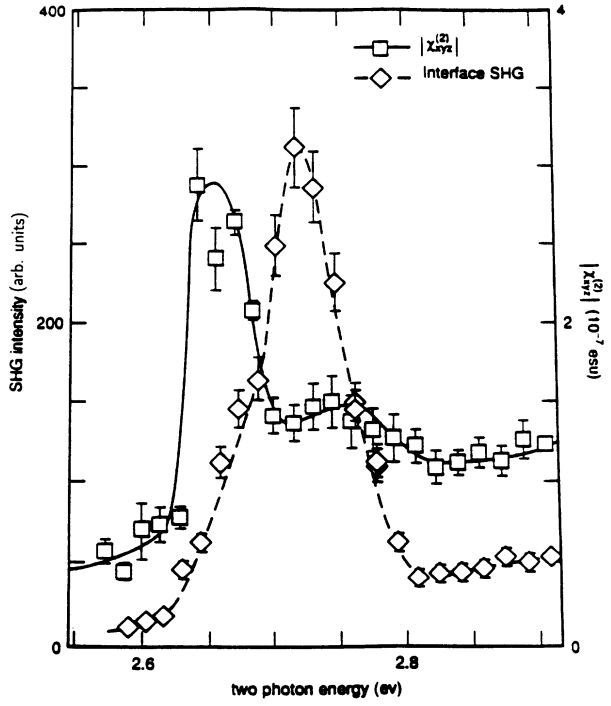

FIG. 12. Deduced $\chi^{(2)}_{xyz}$ of the bulk of the ZnSe overlayer (□) is compared with the interface SH spectrum (◇). The solid lines are only a guide for the eye.

2. *Effect of the photomodulation light on the interfacial SH resonance*

In this section we will discuss the PSHG experiments which were used to confirm the origin of the SH interfacial resonance at 2.72 eV. The underlying mechanism of the PSHG technique can be described as follows. The photogenerating light beam, with photon energy greater than the band gap of the system, produces electron-hole pairs. Some of these free carriers move toward the junction and are captured by the interfacial trap centers, thereby altering the interface charge density. The new interface charge will modify the band bending, and perturb the states associated with the quantum well. The interfacial trapped holes *decrease* the interface negative charge and decrease (increase) the band bending on the ZnSe (GaAs) side of the junction. This delocalizes the quantum well wave function and reduces its relative amplitude within the well and depletion region. The amplitude of the valence band wave function also is reduced within the depletion region of ZnSe overlayer. The decrease in amplitude causes a reduction in the oscillator strength for the transition between the valence band and the quantum well state. Alternatively, interfacial trapped electrons increase the SHG signal.[25]

We have displayed the variation of the interface and bulk signals as a function of lamp intensity using a fixed lamp photon energy of 3.0 eV in Fig. 13. The bulk and the 2.92 eV interface resonance changed by less than 3%, even at the highest lamp powers. In contrast, the 2.72

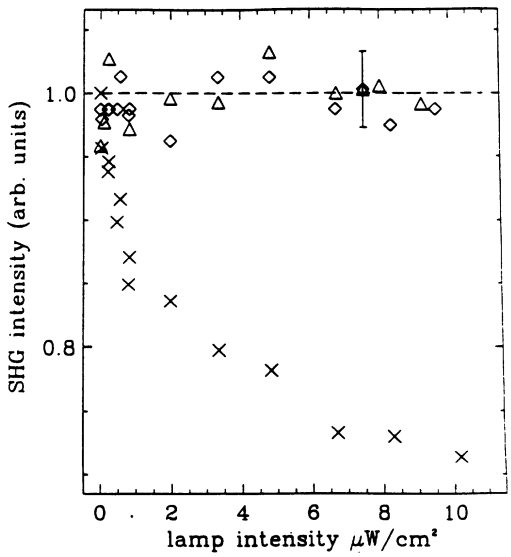

FIG. 13. Normalized variation of the SHG intensity for the interface at 2.72 eV (×) and 2.92 eV (△), and the bulk at 2.67 eV (◇) as a function of the lamp intensity transmitted into the sample at a fixed lamp photon energy of 3.0 eV.

eV interface resonance exhibited a marked decrease in intensity at very low lamp powers. The photomodulation SHG measurements thus lead us to conclude that the two interface resonances at 2.72 eV and 2.92 eV are intrinsically different. This corroborates our earlier assignment of the 2.92 eV resonance to the E_1 transition of buried GaAs. *The photoexcitation was not observed to significantly affect any bulk signal.*

The results of PSHG cannot be explained by the optical pumping of electrons into the quantum well resonance state. Our PSHG data as a function of lamp photon energy, described in Ref. 20, indicate that the maximum rate of change of the SHG intensity occurs at the ZnSe optical band-gap energy of 2.67 eV rather than at 2.72 eV. This fact, along with the observed *increase* of SHG intensity as a result of 2.4 eV carrier-exciting photons, does not support the optical pumping mechanism.[20]

C. Microscopic model of the nonlinear process

We have established that the interfacial SHG resonance at 2.72 eV resulted from a virtual coupling between the ZnSe valence band and the resonance state of the quantum well. However, there are still some interesting problems that remain unsolved quantitatively. For example, what role is played by other bound states in the quantum well, how are the states perturbed by photomodulation, and what type of SH process (i.e., two- or three-level processes) is contributing to the signal. We have constructed a simple theoretical model to study the role of electronic energy levels in the quantum well. This model provides a microscopic picture of the entire process and enables us to quantitatively address the problems above. The computation is based on integration of the one-dimensional Schrodinger equation for the quantum well potential at the heterointerface. The details of this calculation are described in Appendix B. The results and implications of the calculation are given in this section.

TABLE I. Energy levels in the quantum well. Energies are measured relative to the conduction band of ZnSe.

Energy level	Energy (above the ZnSe conduction band)
ε_0	18 meV
ε_1	28 meV
ε_2	54 meV
ε_3	88 meV
ε_4	124 meV
ε_5	159 meV

Wave functions of the first three eigenstates of Eq. (B4) for a sample with an overlayer thickness of 215 Å are shown in Fig. 1, along with the band profile of this system. It should be noted that the well does not have any *bound states*, but carries six distinct *resonance* states above the conduction band of ZnSe. The energy levels of these states are given in Table I.

To identify the resonance state that is responsible for the observed peak at 2.72 eV we must calculate the dipole moment between the valence band state and the quantum well states. This requires knowledge of the wave function of the valence band and we have calculated this wave function in a similar manner (see Fig. 1). The energy of the resultant valence band wave function is equal to the highest value possible within the valence band potential.

The second-order optical susceptibility contains three interband transitions in the three-level SHG process. These transitions, depicted in Fig. 14(a), appear in the numerator of the expression for the second-order susceptibility, $\chi^{(2\omega)}_{ijk}$ i.e.,

$$\chi^{(2)}_{ijk} = -N\frac{e^3}{\hbar^2}\sum_{g,n,n'}\frac{\langle g|r_i|n'\rangle\langle n'|r_j|n\rangle\langle n|r_k|g\rangle}{(2\omega-\omega_{ng}+i\Gamma_{ng})(\omega-\omega_{n'g}+i\Gamma_{n'g})}+\cdots, \tag{8}$$

where $\langle g|$ is the ground state, and $\langle n|$ and $\langle n'|$ are two excited states. In the ZnSe/GaAs(001) system the interfacial SHG resonance at 2.72 eV probably arises through $\chi^{(2\omega)}_{zzz}$.[20] Thus all the matrix elements in Eq. (8) must be determined for $i=j=k=z$, where the z axis is normal to the interface. We have computed the matrix elements of the dipole moment operator using calculated wave functions of the conduction band and the valence band. The result is shown in Fig. 15(a). Our results indicate that the strongest transition dipole occurs between the valence band and the third energy level of the well. The SHG signal is proportional to the square of the matrix element of the dipole moment calculated above. This quantity is displayed in Fig. 15(b) for various energy levels of the quantum well. It is evident that the transition between the valence band and the third resonance state of the quantum well generates the strongest second-harmonic signal in the three-level SHG process, where the other excited state is another conduction band state.

A second-order susceptibility can also involve an intraband transition. In this case the usual three-level process, shown in Fig. 14(a) reduces to a two-level process [see Fig. 14(b)] and the product of the matrix element $\langle g|r_i|n'\rangle\langle n'|r_j|n\rangle\langle n|r_k|g\rangle$ in Eq. (8) is replaced by $|\langle n|z|g\rangle|^2(\mu_g-\mu_{ex})$. Here μ_g and μ_{ex} are the permanent dipole moments of the ground state and excited state of the system, respectively. This type of process was suggested by Burstein, Pajer, and Pinczuk,[33] and used to explain the second-order nonlinear spectrum of Cu(110).[34,35] Since the symmetry of the system near the junction in the direction normal to the heterointerface of the ZnSe/GaAs(001) is broken by band bending, the intraband transition is an allowed transition within the quantum well states. Therefore, a two-level SHG process at the interface of ZnSe/GaAs(001) can also occur. The first step of this process is an interband transition from the valence band of the ZnSe to the resonance state of the

quantum well. An intraband transition in the resonance state of the well is the second step, and the last step is an interband transition from the quantum well state back to the valence band.

Now we assume that the SHG process, responsible for the interfacial resonance at 2.72 eV, is a two-level process. We must calculate the relative oscillator strength of the signal for each quantum well state, namely

$$\{|\langle\phi_v|z|\phi_{\text{well}}\rangle|^2(\mu_g-\mu_{\text{ex}})\}^2, \tag{9}$$

where

$$\mu_g=\langle\phi_v|z|\phi_v\rangle \tag{10}$$

and

$$\mu_{\text{ex}}=\langle\phi_{\text{well}}|z|\phi_{\text{well}}\rangle. \tag{11}$$

Here $\langle\phi_v|$ and $\langle\phi_{\text{well}}|$ are the wave functions of the valence band and the interfacial quantum well, respectively. The difference between these two permanent dipole moments, which we shall refer to as the permanent dipole moment of the system, is shown in Fig. 16(a) for each state in the well. The relative SHG intensity in a two-level process for various quantum well states is displayed in Fig. 16(b). It is clear that the third energy level in the quantum well is the strongest contributor to the SHG signal. This level is about 50 meV above the conduction band of ZnSe and is in good agreement with experimental results. The permanent dipole moment of the system, shown in Fig. 16(a), is at least an order of magnitude greater than the transition dipole moment between the valence band and the interfacial quantum well states (Fig. 15). Based on this comparison we speculate that the permanent dipole moment is still stronger than any transition dipole moment involving the quantum well states and other conduction band states. Thus, the product of the matrix elements involved in the two-level SHG process is greater than the product of the matrix elements involved in the three-level process, and the second-order susceptibility in the two-level process is stronger than the second-order susceptibility in the three-level process.[36] This picture suggests that the interfacial resonance at 2.72 eV is a result of a two-level SHG process.

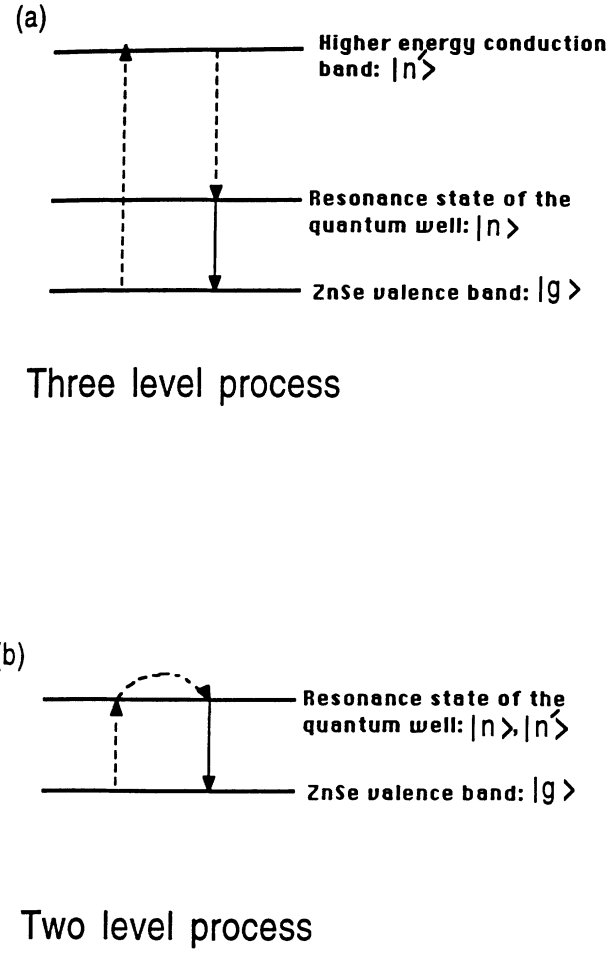

FIG. 14. (a) Possible three-level process in the ZnSe/GaAs heterointerface. (b) Two-level process in the ZnSe/GaAs heterointerface.

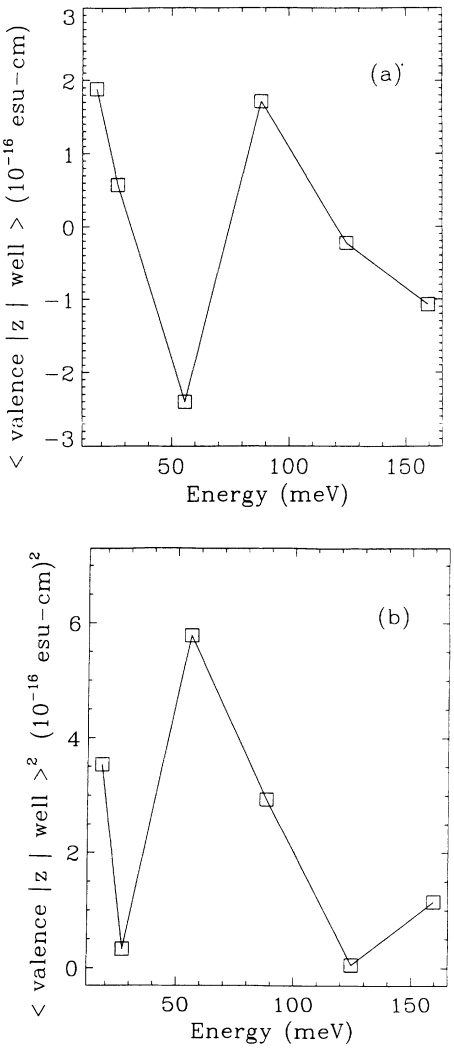

FIG. 15. (a) Calculated matrix element of the dipole moment as a function of the energy for the interfacial quantum well. It is clear that the third energy level generated the strongest matrix element. (b) Square of the calculated matrix element.

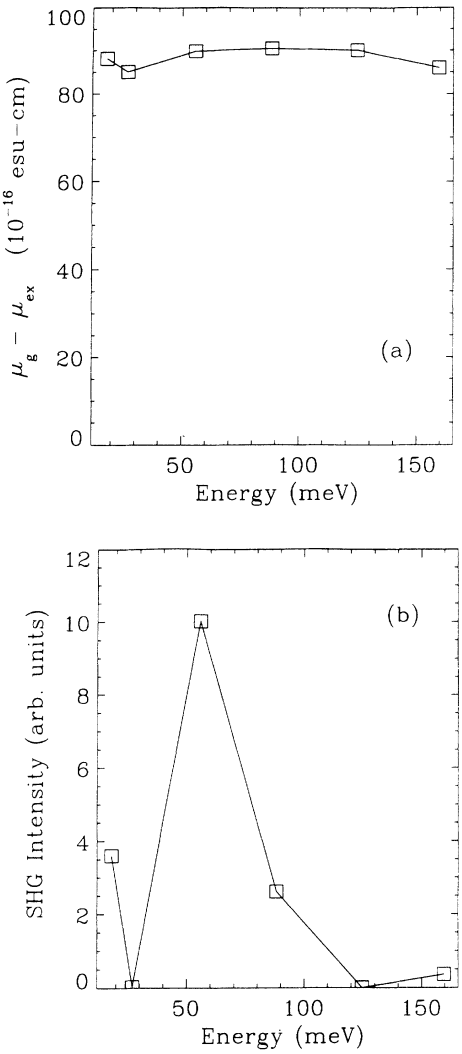

FIG. 16. (a) Calculated permanent dipole moment of the system, $\mu_g - \mu_{ex}$, as a function of the energy level in the interfacial quantum well. (b) Relative strength of the SH signal as a function of energy in the two-level process.

IV. CONCLUSION

We have used second-harmonic and sum-frequency spectroscopy to probe the electronic structure of the interface and bulk of ZnSe/GaAs(001) heterostructures. We were able to separate the bulk and interface contributions by proper choice of polarization and sample orientation. The interface of ZnSe/GaAs(001) systems exhibited strong SH and SF resonances at 2.92 and 2.72 eV. The 2.92 eV resonance was assigned to the E_1 transition of buried GaAs. The spectral feature at 2.72 eV was produced as a result of virtual coupling between the ZnSe valence band and a *resonance state* of a quantum well located *across* the junction in the GaAs conduction band. The interfacial quantum well was brought about by interdiffusion of Zn into GaAs and Ga into ZnSe during sample growth.

Linear photomodulation and second-harmonic generation were combined as a method to investigate solid-solid interfaces. Using this technique, we have studied the effect of the band flattening on the interfacial resonance at 2.72 eV. The sensitivity of the resonance to the variation of the band profile near the junction confirms that the signal is from coupling to the resonance state of the quantum well.

A microscopic calculation of the effect indicates that the most probable mechanism for the resonance arises between the valence band and the third resonance state of the quantum well. The same computation also suggested that the nonlinear process involves an intraband transition within the quantum well resonance. This process involves only two energy levels.

ACKNOWLEDGMENTS

We would like to thank E. Burstein, E. Borguet, H. H. Farrell, J. W. Garland, P. D. Kaplan, I. Koltover, E. J. Mele, R. E. Nahory, E. W. Plummer, S. Rabii, P. M. Raccah, and W. Theis for stimulating discussions, and A. Denenstein for technical help. This work was supported by the ONR through its Young Investigator program No. N00014-91-J-1867. A.G.Y. also acknowledges partial support from the NSF through the MRL program No. DMR-8519059, and the Alfred P. Sloan Foundation.

APPENDIX A: ENERGY SHIFT BY DEFORMATION POTENTIAL

We start the computation with the orbital-strain perturbation Hamiltonian H_ϵ for tetragonal symmetries introduced by Pikus and Bir,[37]

$$H_\epsilon = -a(\epsilon_{xx} + \epsilon_{yy} + \epsilon_{zz}) - 3b[(L_x^2 - \tfrac{1}{3}L^2)\epsilon_{xx} + \text{c.p.}], \tag{A1}$$

where ϵ_{ij} represents the components of the strain tensor and L is the angular-momentum operator. "c.p." denotes cyclic permutation with respect to the indices x, y, and z. The parameters a and b are the hydrostatic and shear potential, respectively. For biaxial stress parallel to the [100] and [010] directions, the strain tensor is

$$\epsilon = \begin{pmatrix} -\epsilon & 0 & 0 \\ 0 & -\epsilon & 0 \\ 0 & 0 & 2\epsilon C_{12}/C_{11} \end{pmatrix}, \tag{A2}$$

where C_{ij} stands for the elastic stiffness of the ZnSe overlayer. This reduces the Hamiltonian to

$$H_\epsilon = 2a\epsilon\left(1 - \frac{C_{12}}{C_{11}}\right) - 3b\epsilon\left(1 + \frac{2C_{12}}{C_{11}}\right)(L_z^2 - \tfrac{1}{3}L^2). \tag{A3}$$

Gavini and Cardona[38] calculated the eigenvalue of this strain Hamiltonian using the unperturbed wave functions of the valence and conduction bands in zinc blende materials. Their perturbation calculations predict an energy shift between the valence band and the conduction band at the center of the Brillouin zone. These energy shifts are

$$\Delta E_0(1) = \left[-2a\left(\frac{C_{11}-C_{12}}{C_{11}}\right) + b\left(\frac{C_{11}+2C_{12}}{C_{11}}\right)\right]\epsilon, \tag{A4}$$

$$\Delta E_0(2) = \left[-2a\left(\frac{C_{11}-C_{12}}{C_{11}}\right) - b\left(\frac{C_{11}+2C_{12}}{C_{11}}\right)\right]\epsilon, \tag{A5}$$

and

$$\Delta(E_0+\Delta_0) = -2a\left(\frac{C_{11}-C_{12}}{C_{11}}\right)\epsilon, \tag{A6}$$

where $\Delta E_0(1)$, $\Delta E_0(2)$, and $\Delta(E_0+\Delta_0)$ are the energy shifts between the valence bands and conduction band (see Fig. 11). Taking $C_{11} = 0.826 \times 10^6$ kg/cm^2, $C_{12} = 0.498 \times 10^6$ kg/cm^2, $a = -4.25$ eV, $b = -0.40$ eV, and $\epsilon = 3.0 \times 10^{-3}$,[39] we deduce the energy shifts to be

$$\Delta E_0(1) = 7.0 \text{ meV},$$

$$\Delta E_0(2) = 13.0 \text{ meV},$$

and

$$\Delta(E_0+\Delta_0) = 10.0 \text{ meV}.$$

Thus the measured energy shift between the interface and bulk susceptibilities is ~ 4 times too large to be attributed to the strain-induced shift.

APPENDIX B: ELECTRONIC ENERGY LEVELS IN THE INTERFACIAL QUANTUM WELL

Electronic motion is governed by the Schrödinger equation[40]

$$-\frac{\hbar^2}{2}\nabla\frac{1}{m(r)}\nabla\psi(r) + V(r)\psi(r) = \varepsilon\psi(r). \tag{B1}$$

If an electron is free in the plane parallel to the interface (i.e., the xy plane), the potential is

$$V(r) = V(z), \tag{B2}$$

where z is zero at the surface of the ZnSe and is equal to d at the interface. This leads to a wave function of the form

$$\psi(r) = \frac{1}{\sqrt{A}}e^{i(k_x x + k_y y)}\phi(z), \tag{B3}$$

where A is the sample area. With $k_x = k_y = 0$ Eq. (B1) reduces to

$$-\frac{\hbar^2}{2}\frac{\partial}{\partial z}\frac{1}{m(z)}\frac{\partial}{\partial z}\phi(z) + V(z)\phi(z) = \varepsilon\phi(z), \tag{B4}$$

with

$$m(z) = \begin{cases} m_{\text{ZnSe}} & \text{if } z < d; \\ m_{\text{GaAs}} & \text{if } z > d. \end{cases} \tag{B5}$$

The continuity condition states that $\phi(z)$ and $[1/m(z)][\partial\phi(z)/\partial z]$ must be continuous at the junction of ZnSe and GaAs.[41] We rewrite Eq. (B4) in a dimensionless form for each side of the junction,

$$\frac{\partial^2\phi(\zeta)}{\partial\zeta^2} = (e-v)\bar{m}_*\phi(\zeta), \tag{B6}$$

with

$$\frac{z}{\zeta} = 10 \times a_0 \text{ where } a_0 = 0.529\ \mathring{A}, \tag{B7}$$

$$\bar{m}_* = \frac{m}{10m_e}, \text{ and } R_y a_0^2 = \frac{\hbar^2}{2m_e},$$

and also

$$\frac{\varepsilon}{e} = mR_y, \ \frac{V}{v} = mR_y \text{ where } mR_y = 13.605 \text{ meV}.$$

We solved this dimensionless Schrödinger equation numerically for the potential $V(z)$, depicted in Fig. 1.[42] The potential was derived as follows. The value $\Phi(z) = -V(z)/e$ is the outcome of Poisson's equation for interfacial charge distribution. Kassel *et al.*[10] showed that the charge distribution at the interface can be described by a Gaussian function. In ZnSe, the charge distribution is

$$\rho(z)_{\text{ZnSe}} = \frac{eN_{\text{ZnSe}}}{\lambda_{\text{Ga}}\sqrt{2\pi}}\exp\left(-\frac{(z-d)^2}{2\lambda_{\text{Ga}}^2}\right). \tag{B8}$$

A similar charge distribution is written for the GaAs side of the junction,

$$\rho(z)_{\text{GaAs}} = \frac{-eN_{\text{GaAs}}}{\lambda_{\text{Zn}}\sqrt{2\pi}}\exp\left(-\frac{(z-d)^2}{2\lambda_{\text{Zn}}^2}\right), \tag{B9}$$

where N is the number density of the charge and λ is the diffusion length. To solve Poisson's equation,

$$-\nabla^2\Phi = \frac{1}{\epsilon}\rho, \tag{B10}$$

we use two boundary conditions on each side of the junction, namely $\Phi_{\text{junction-ZnSe}}$ and $\Phi_{\text{surface-ZnSe}}$ for the ZnSe side, and $\Phi_{\text{junction-GaAs}}$ and $\Phi_{\text{bulk-GaAs}}$ for the GaAs side. Then we solve Eq. (B10) numerically. In this numerical method we have divided the distance coordinate z into a "mesh" of small segments of equal width δz. Following the conventional form for the parameters at the jth mesh point

TABLE II. Parameters used for band-profile calculations

Parameter	Value of the parameter
N_{Ga}	8.5×10^{12} cm^{-2}
N_{Zn}	5.1×10^{12} cm^{-2}
λ_{Ga}	4 nm
λ_{Zn}	10 nm
$\Phi_{\text{ZnSe surface}}$	100 meV
$\Phi_{\text{ZnSe interface}}$	180 meV
$\Phi_{\text{GaAs interface}}$	370 meV

$$z \to z_j \equiv j\delta z,$$

$$\Phi(z) \to \Phi(z_j) \equiv \Phi_j,$$

$$\rho(z) \to \rho(z_j) \equiv \rho_j,$$

we can calculate Φ_{j+1} as a function of Φ_j and Φ_{j-1}, i.e.,

$$\Phi_{j+1} = 2\Phi_j - \Phi_{j-1} - \rho'_j, \tag{B11}$$

where Φ_j is the value of Φ at the jth mesh point and ρ' is $(\delta z)^2\rho/\epsilon$ with mesh size δz. If we start the calculation from the surface of the ZnSe ($j = 0$), then we need to know the value of Φ_1. One can show that

$$\Phi_j = j\Phi_1 - (j-1)\Phi_0 - [(j-1)\rho'_1 + (j-2)\rho'_2 + \cdots + \rho'_{j-1}]. \tag{B12}$$

This gives the value of Φ_1 as a function of two boundary conditions Φ_0 and Φ_M, that is

$$\Phi_1 = \{\Phi_M + (M-1)\Phi_0 + [(M-1)\rho'_1 + \cdots]\}/M, \tag{B13}$$

where M defines the last mesh point. The potential $V = -e\Phi$ for the valence band and the conduction band are shown in Fig. 1. The parameters used for this computation are tabulated in Table II.

*Present address: Exxon Research and Engineering Co., Clinton Township, NJ 08801.

[1] See, for example, T. F. Heinz in *Nonlinear Surface Electromagnetic Phenomena*, edited by H. E. Ponath and G. I. Stegeman (Elsevier Science Publisher B.V., Amsterdam, 1991); Y. R. Shen, Annu. Rev. Phys. Chem. **40**, 327 (1989).

[2] J. F. McGilp and Y. Yeh, Solid State Commun. **59**, 91 (1986); J. F. McGilp, J. Vac. Sci. Technol. A **5**, 1442 (1987); J. Phys. Condens. Matter **1**, SB85 (1989).

[3] T. F. Heinz, F. J. Himpsel, E. Palange, and E. Burstein, Phys. Rev. Lett. **63**, 644 (1989); F. J. Himpsel, T. F. Heinz, A. B. Mclean, and E. Palange, Appl. Surf. Sci, **41**, 346 (1989).

[4] J. C. Hamilton, R. T. Tung, and H. W. K. Tom, *Quantum Electronics Laser Science, 1991 Conference Edition* (Optical Society of America, Washington, D.C., 1991), p. 30.

[5] M. S. Yeganeh, J. Qi, A. G. Yodh, and M. C. Tamargo, Phys. Rev. Lett. **68**, 3761 (1992).

[6] M. S. Yeganeh, J. Qi, A. G. Yodh, and M. C. Tamargo, Phys. Rev. Lett. **69**, 3579 (1992).

[7] G. Lupke, D. J. Bottomley, and H. M. van Driel, Phys. Rev B, **47**, 10 389 (1993).

[8] W. Daum, H. J. Hrause, U. Reichel, and H. Ibach, Phys. Rev. Lett. **71**, 1234 (1993).

[9] M. A. Haase, J. Qiu, J. M. Depuydt, and H. Cheng, Appl. Phys. Lett. **59**, 1272 (1991).

[10] L. Kassel, H. Abad, J. W. Garland, P. M. Raccah, J. E. Potts, M. A. Haase, and H. Cheng, Appl. Phys. Lett. **56**, 42 (1990).

[11] E. Y. Wang, W. A. Albers, and C. E. Bleil, in *II-VI Semiconducting Compounds*, edited by D. G. Thomas (Benjamin, New York, 1967), p. 136.

[12] R. E. Nahory and J. L. Shay, Phys. Rev. Lett. **21**, 1569 (1968).

[13] For details of sample growth and morphology, see M. C. Tamargo, J. L. deMiguel, D. M. Hwang, and H. H. Farrell, J. Vac. Sci. Technol. B **6**, 784 (1988), and references therein.

[14] M. C. Tamargo, R. Nahory, B. J. Skromme, S. M. Shibli, A. L. Weaver, R. J. Martine, and H. H. Farrell, J. Cryst. Growth, **111**, 741 (1991).

[15] R. M. Park, H. A. Mar, and N. M. Salansky, J. Vac. Sci. Technol. B **3**, 676 (1985); R. L. Longini, Solid-State Electron. **5**, 127 (1962).

[16] Y. Z. Liu, R. J. Anderson, R. A. Milano, and M. J. Cohen, Appl. Phys. Lett. **40**, 967 (1982).

[17] H. Kroemer, J. Appl. Phys. **52**, 873 (1980).

[18] R. People, K. W. Wecht, K. Alavi, and A. Y. Cho, Appl. Phys. Lett. **43**, 118 (1983).

[19] P. D. Maker, R. W. Terhune, M. Nisenoff, and C. M. Savage Phys. Rev. Lett. **8**, 21 (1962); J. Jerphagnon and S. K. Kurtz, J. Appl. Phys. **41**, 1667 (1970).

[20] M. S. Yeganeh, J. Qi, A. G. Yodh, and M. C. Tamargo, J. Opt. Soc. Am. B **10**, 2093 (1993).

[21] See, for example, Y.R. Shen, *The Principles of Nonlinear Optics* (Wiley-Interscience, New York, 1984).

[22] T. Stehlin, M. Feller, P. Guyot-Sionnest, and Y. R. Shen, Opt. Lett. **13**, 389 (1988).

[23] M. S. Yeganeh, J. Qi, J. P. Culver, A. G. Yodh, and M. C. Tamargo, Phys. Rev. B **46**, 1603 (1992).

[24] The 2.72 and 2.92 eV resonances are *virtual* transitions in that there is never any population transferred between the ground state and excited states. This is evident from the fact that the input photons have energy well within the semiconductor band gaps.

[25] M. S. Yeganeh, Ph.D. thesis, University of Pennsylvania, 1992.

[26] B. O. Seraphin and H. E. Bennett, *Semiconductors and Semimetals* (Academic, New York, 1967), Vol. 3.

[27] M. Aven, D. T. F. Marple, and B. Segall, J. Appl. Phys. **32**, 2261 (1961).

[28] D. E. Aspnes and A. A. Studna, Phys. Rev. B **27**, 985 (1983).

[29] P. Dawson, R. A. Wilson, C. W. Tu, and R. C. Miller, Appl. Phys. Lett. **48**, 541 (1986).

[30] S. J. Hsieh, E. A. Patten, and C. M. Wolfe, Appl. Phys. Lett. **45**, 1125 (1984).

[31] P. Voision, G. Bastard, C. E. T. Goncalves da Silva, M. Voos, L. L. Chang, and L. Esaki, Solid State Commun. **39**, 79 (1981).

[32] H. Asai, and K. Oe, J. Appl. Phys. **54**, 2052 (1983).

[33] E. Burstein, G. Pajer and A. Pinczuk, in *Proceedings of the International Conference on the Physics of Semiconductors, Stockholm, 1986*, edited by O. Engstrom (World Scientific, Singapore, 1987), p. 1691.

[34] M. Y. Jiang, Ph.D. thesis, University of Pennsylvania, 1992; M. Y. Jiang, G. Pajer, E. Burstein, M. S. Yeganeh, and A. G. Yodh, Bull. Am. Phys. Soc. **37**, 652 (1992).

[35] Because of similarity between Cu(110) and Ag(110), the two-level SHG process could also be used to explain the second-order nonlinear spectrum of Ag(110) studied by L. E. Urbach, K. L. Percival, J. M. Hicks, E. W. Plummer, and H. L. Dai, Phys. Rev. B **45**, 3769 (1992).

[36] In contrast to the three-level SHG process, the energy difference between the intermediate excited states is zero in the two-level SHG process. However, this only affects the nonresonant terms of $\chi^{(2\omega)}_{ijk}$. It has no significant impact for

distinguishing two- and three-level SHG processes.
[37]G. E. Pikus and G. L. Bir, Sov. Phys. Solid State **1**, 136 (1959); **1**, 1502 (1960).
[38]A. Gavini and M. Cardona, Phys. Rev. B **1**, 672 (1970).
[39]D. Berlincourt, H. Jaffe, and L. R. Shiozawa, Phys. Rev. **129**, 1009 (1963); Y. F. Tsay, S. S. Mitra, and B. Bendow, Phys. Rev. B **10**, 1476 (1974); D. W. Langer, R. N. Euwema, K. Era, and T. Koda, ibid. **2**, 4005 (1970).
[40]C. Weisbuch and B. Vinter, *Quantum Semiconductor Structures: Fundamentals and Applications* (Academic Press, Boston, 1991); G. Bastard, *Wave Mechanics Applied to Semiconductor Heterostructures* (Halsted Press, New York, 1988).
[41]H. C. Liu, Superlatt. Microstruc. **3**, 413 (1987); P. Enders, Phys. Status Solidi B **139**, K113 (1987); R. A. Morrow and K. R. Brownstein, Phys. Rev. B **30**, 678 (1984); R. Morrow, *ibid.* **35**, 8074 (1987); **36**, 4836 (1987); J. Thomsen, G. T. Einevoll, and P. C. Hemmer, *ibid.* **39**, 12 783 (1989); I. Galbraith and G. Duggan, **38**, 10 057 (1988).
[42]A. P. French and E. F. Taylor, *An Introduction to Quantum Physics* (W. W. Norton, New York, 1987).